BNL-94679-2011-TECH

BNL-94679-2011-IR

Effect of the electron lenses on the RHIC proton beam closed orbit

X. Gu,

February 2011

Collider Accelerator Department

Brookhaven National Laboratory

U.S. Department of Energy

USDOE Office of Science (SC)

DISCLAIMER

BNL-94679-2011-IR

C-A/AP/#424
Feb. 2011

Effect of the Electron Lenses on the RHIC Proton Beam Closed Orbit

X. Gu, Y. Luo, A. Pikin, M. Okamura, W. Fischer, C. Montag,
R. Gupta, J. Hock, A. Jain, D. Raparia

Collider-Accelerator Department
Brookhaven National Laboratory
Upton, NY 11973

Effect of the Electron Lenses on the RHIC Proton Beam Closed Orbit

X. Gu, Y. Luo, A. Pikin, M. Okamura, W. Fischer, C. Montag, R. Gupta, J. Hock, A. Jain, D. Raparia

Brookhaven National Laboratory, Upton, NY 11973

December 30, 2010

Abstract

We are designing two electron lenses (E-lens) to compensate for the large beam-beam tune spread from proton-proton interactions at IP6 and IP8 in the Relativistic Heavy Ion Collider (RHIC). They will be installed at RHIC IR10. The transverse fields of the E-lenses' bending solenoids and the fringe field of the main solenoids will shift the proton beam. We calculate the transverse kicks that the proton beam receives in the electron lens via Opera. Then, after incorporating the simplified E-lens lattice in the RHIC lattice, we obtain the closed orbit effect with the Simtrack Code.

1. Introduction

The Relativistic Heavy Ion Collider (RHIC) at Brookhaven National Laboratory has operated for a decade. It has two rings in a horizontal plane with two head-on beam-beam interactions (IP6 and IP8) and four long-range beam-beam interactions.

The proton beam in the Blue ring circulates clockwise, while that in the Yellow ring circulates anti-clockwise. In long-range beam-beam interactions the beam are separated vertically by 10 mm. The current beam pipe at IP10 has a 65 mm radius.

Like in other colliders, the beam-beam interaction limits the luminosity of RHIC's polarized proton operation. To compensate for the large beam-beam tune spread due to head-on proton-proton interactions at IP6 and IP8 in RHIC, we are designing two E-lenses that we will install between the two DX dipoles at RHIC IR10. Here, we discuss the layout of these two E-lenses.

Furthermore, to clarify the effects of such electron lenses on RHIC's proton beam, we detail the layout of the RHIC lattice that includes the simplified E-lens lattice (Figure 1). Then, with this lattice in place, we evaluated, via the Simtrack code, the proton beam's closed orbit, its beta functions and its phase advance at IR10.

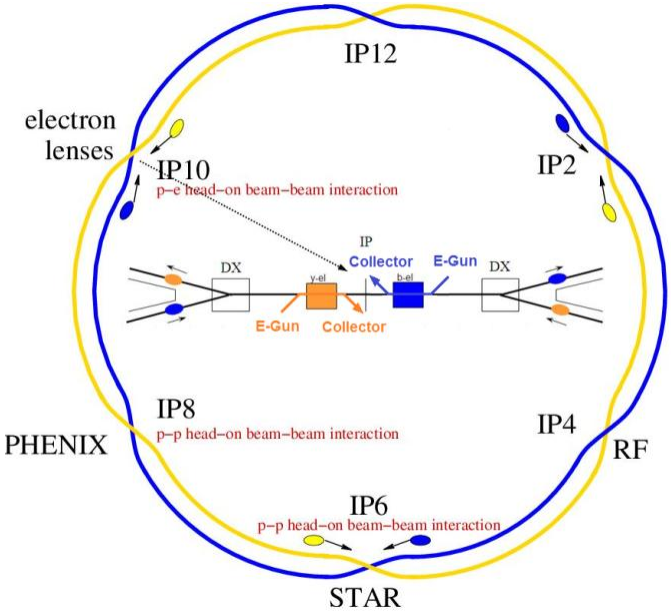

Figure 1: Layout of RHIC and of the E-lenses

2. The Layout of the Two Electron Lenses

Each of RHIC's E-lenses has one DC electron gun, one main superconducting magnet, one electron collector, and a beam transport system. This beam transport system has six solenoids, from the gun side to the collector side, viz., GS1, GS2, GSB, CSB, CS2, and CS1. To avoid affecting the DC electron guns with an unwanted electromagnetic field, we placed two DC electron guns away from the IP, while the two collectors are located near the IP (Figure 1).

Furthermore, to compensate for head-on beam-beam collision, the direction of the electron beam must be opposite that of the proton beam so that the electric and magnetic forces add. This means that when the E-lenses are operating, the ring's blue (yellow) proton beam must pass first through the yellow (blue) electron lenses. At this time, the blue (yellow) proton beam is being transported in the same direction as the yellow (blue) electron beam, but separated from it vertically by 10 mm. Then, the blue (yellow) proton beam continues, progressing through the blue (yellow) electron lens, so that its transport direction is opposite that of the blue (yellow) electron beam.

Also, due to the 10 mm vertical separation between the two proton beams, the electron beams must be separated similarly. Two layouts of the E-lens can meet this requirement. First, we can set the vertical center of the two electron lenses at the same vertical position (i.e., the center of vacuum pipe, Y=0), and use steering magnets to move the electron beam either up by 5mm, or down by 5 mm. We can achieve the same outcome mechanically, offsetting one of the electron lenses by 5mm up from Y=0, and the other 5mm down. Then, the electron beam will interact head-on with the proton beam. The latter

approach, the mechanical one, does not entail having magnets to move the electron beam 5 mm up and down, and so, it is easier to control.

Figure 2 shows the configuration of the magnetic structure of the two electron lenses with these constraints. The electron beam in one electron lens interacts head-on only with one proton beam.

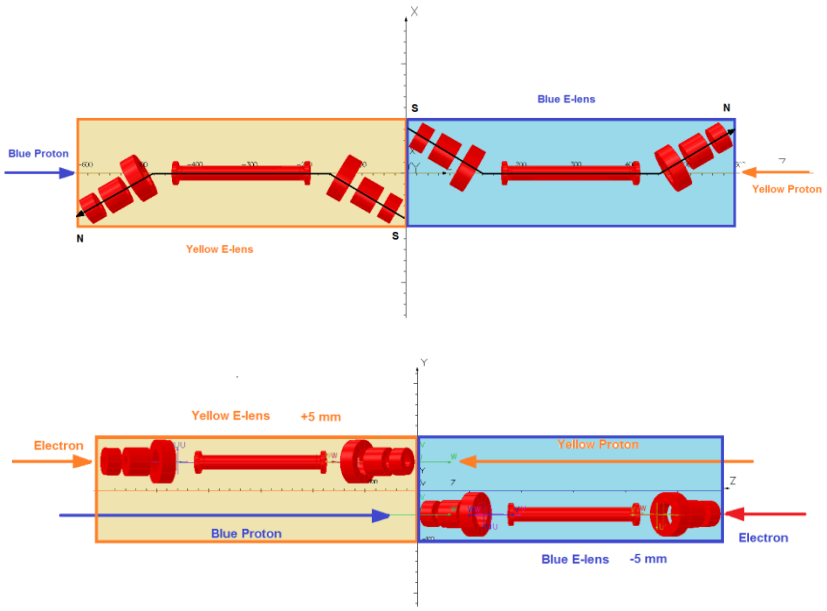

Figure 2: Layout of Two Electron Lenses. Top: top view, bottom: side view.

In addition to these constraints, the two lenses should have a different magnetic polarity (SN-NS or NS-SN) and therefore, locally compensate each other for both linear coupling and spin effects. Furthermore, the center line of the solenoids GSB_Y, CSB_Y, CSB_B, and GSB_B, located, respectively, at -490cm, -145 cm, 145 cm, and 490 cm have a 30 degree angle between the directions of proton-beam transport. This configuration will induce high-order magnetic-field components when the proton beam passes through the two E-lenses; Figure 3 illustrates these components of two electron lenses along the center of the vacuum pipe.

The multipole magnetic field components in Fig. 3 generated by E-lens are analyzed and compared by Fourier fit method.

In cylindrical coordinates, we can express the radial and azimuthal components of magnetic field B in the form:

$$\mathrm{B_r}(\mathrm{r},\theta) = \sum_{n=1}^{\infty}(b_n \sin(\mathrm{n}\theta) + a_n \cos(\mathrm{n}\theta)) \qquad (1)$$

$$\mathrm{B_\theta}(\mathrm{r},\theta) = \sum_{n=1}^{\infty}(b_n \sin(\mathrm{n}\theta) - a_n \cos(\mathrm{n}\theta)) \qquad (2)$$

Where b_n is the amplitudes of the $2n$ pole normal term and a_n is the amplitudes of $2n$ pole skew term in the "European Convention".

The multipole magnetic field, B_θ can be computed on a reference radius R_{ref} at different longitudinal positions and fitted as Fourier series. Then, according to formula (2), the coefficients of this Fourier series are the multipole magnetic field components. The reference radius R_{ref} = 75 mm.

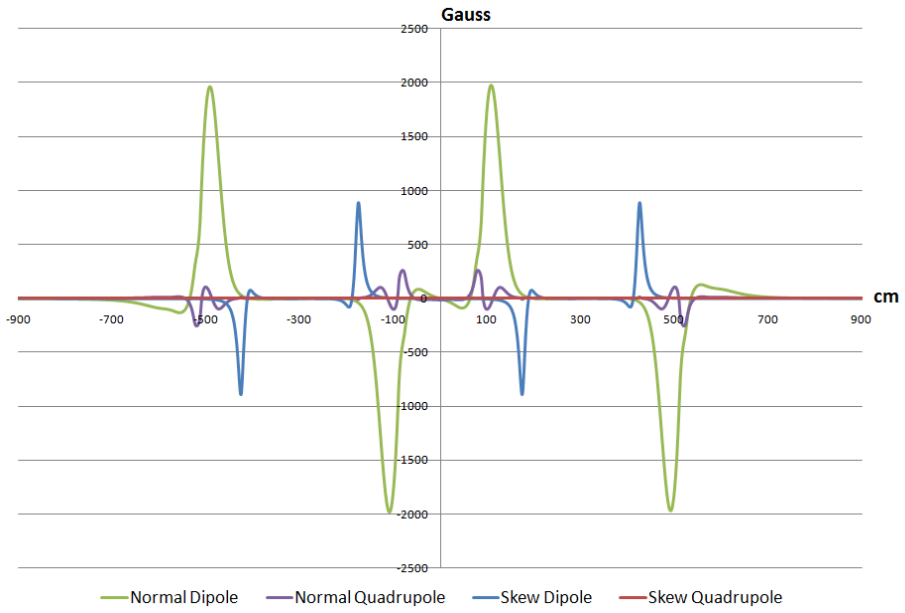

Figure 3: High-Order Magnetic Field Components.

3. Single-pass Trajectories of the Proton Beam Tracked by Opera

The dipole component field of the two electron lenses can deflect the trajectories of protons. To verify this effect and find a method to correct it, we tracked, by Opera, the centroid of the blue proton beam as it passed through these two electron lenses.

In our simulation, the blue proton beam starts from -900 cm with eight different initial vertical angles; the horizontal angle is set to zero. The energy of the proton beam is 250 GeV, and the Lorentz factor is 266.

Figure 4 reveals that the blue proton beam has the same angle before and after the two electron lenses. However, within them, the blue proton beam is deflected. If its initial angle is about 100 μrad, the blue proton beams' trajectories within the two electron lenses can be set to be parallel to the Z-axis.

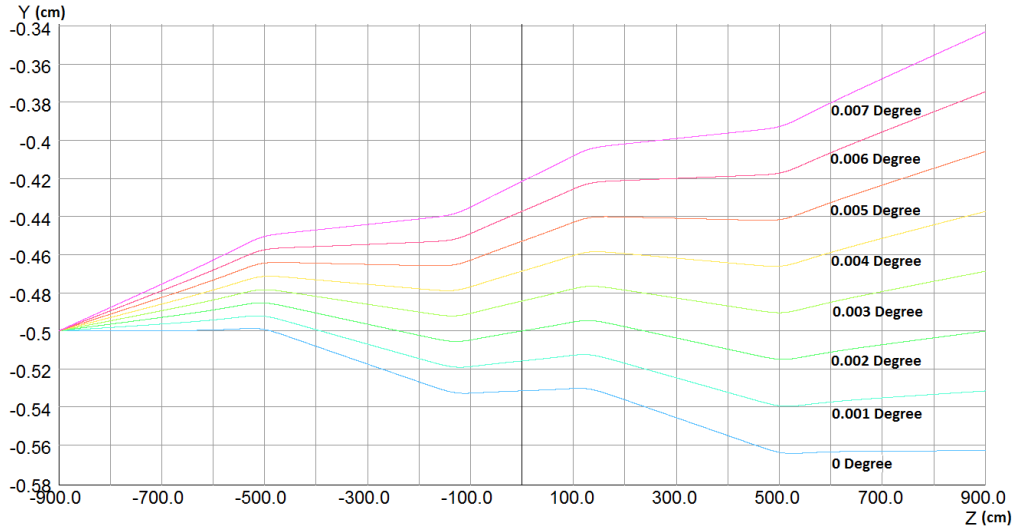

Figure 4: Proton Beam's Vertical Trajectories in Electron Lenses.

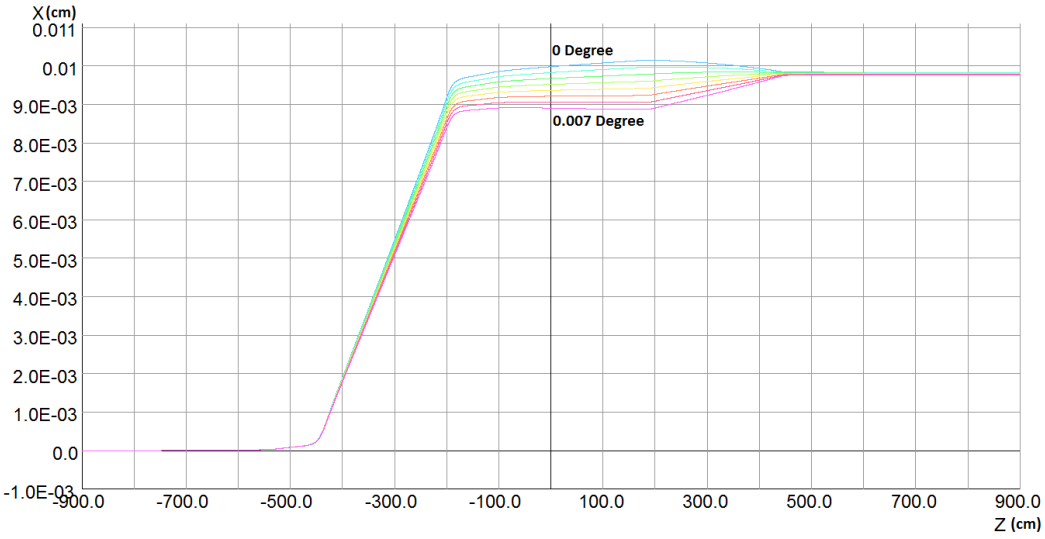

Figure 5: Proton Beam's Horizontal Trajectories in Electron Lenses.

Figure 5 plots the blue proton beam's horizontal trajectories. After passing through the two electron lenses, it exhibits a shift of about 0.01 cm. Because the blue proton beam passes first through the yellow 5 mm E-lens, it is deflected by the fringe field of the yellow E-lens by about 0.009 cm; this value is much greater than the change in the beam's position caused by the fringe field of the blue E-lens, which is less than 0.001 cm.

4. Simplification of the Electron Lenses' Lattice

To include the E-lenses' elements lattice in the RHIC lattice, these elements, such as the transverse field of GSB and the fringe field of the main solenoid, must be simplified and replaced by an element that can be used in some tracking codes, such as Simtrack.

In this paper, for simplification, we consider only the dipole components of the E-lenses' lattice, neglecting all higher order components.

Figure 6 and Figure 7 respectively, plot the transverse field of the GSB and the fringe field of main solenoid. In Figure 6 the horizontal field Bx was plotted for the line (0, 0, Z) cm and (1, 1, Z) cm (the red line); Z is from -700 cm to -400 cm. The two plots show only a slight difference. It is also confirmed that the vertical distribution of the Bx field does not change. Therefore, we assumed that Bx is constant in the XY plane.

In Figure 7 the vertical field By was plotted for the line (0, -0.4, Z) cm (the red line) and (0, -0.6, Z) cm; Z is from -735 cm to -435 cm. When the elements of the electron lenses are simplified, By is also assumed to be uniform in the XY plane; even there is about 20% difference between Bx and By at the peak point of the field.

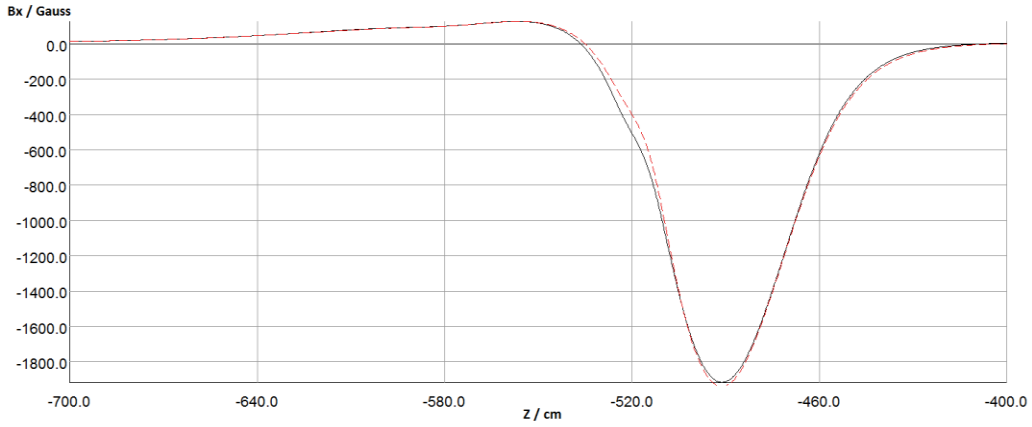

Figure 6: Bx field.

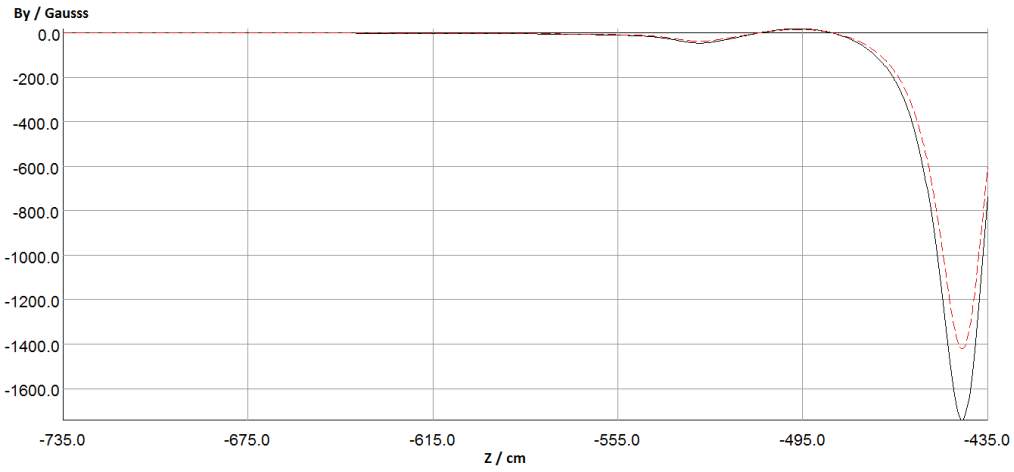

Figure 7: By Field

Since the fields Bx and By are assumed to be uniform fields in transverse plane, we also assumed that they are generated by many X dipoles and Y dipoles along the Z axis. In the Simtrack code, we can

represent the X and Y dipoles at the same longitudinal position by a KICKER element, which has a vertical and a horizontal kicker force.

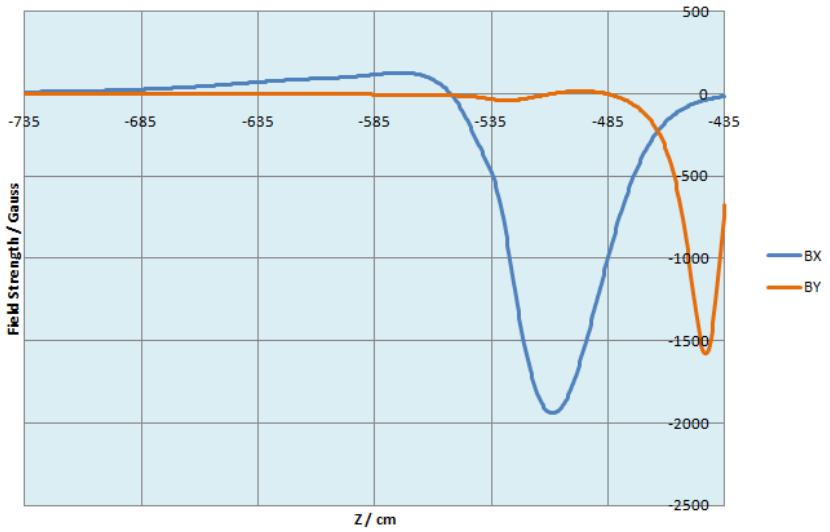

Figure 8: The Magnetic Field from -735 cm to -435 cm.

Figure 8, Figure 9 and Figure 10, respectively, are the magnetic fields between (-735, -435) cm, (-200, 200) cm, and (435, 735) cm along (0, -0.5, Z) cm. In the Simtrack code, these magnetic fields are represented, separately, by 30-, 40-, and 30-KICKERs; each KICKER is 10 cm long.

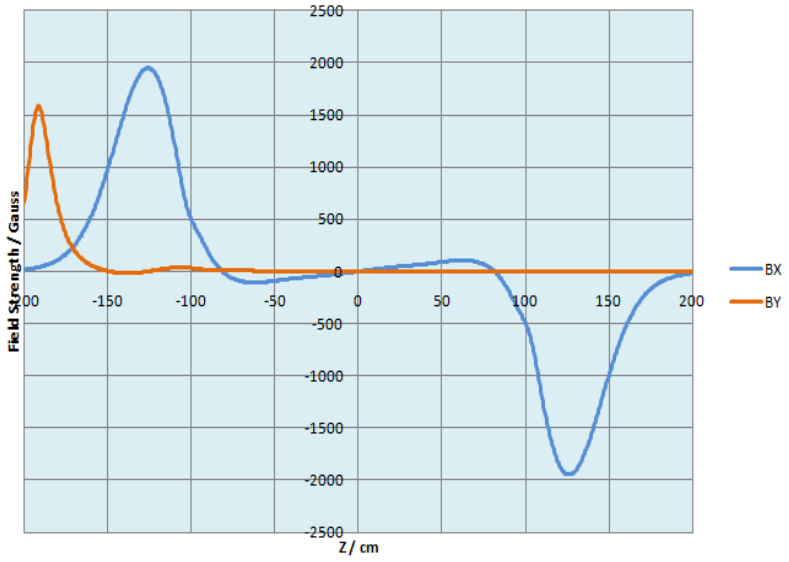

Figure 9: The Magnetic Field from -200 cm to +200 cm

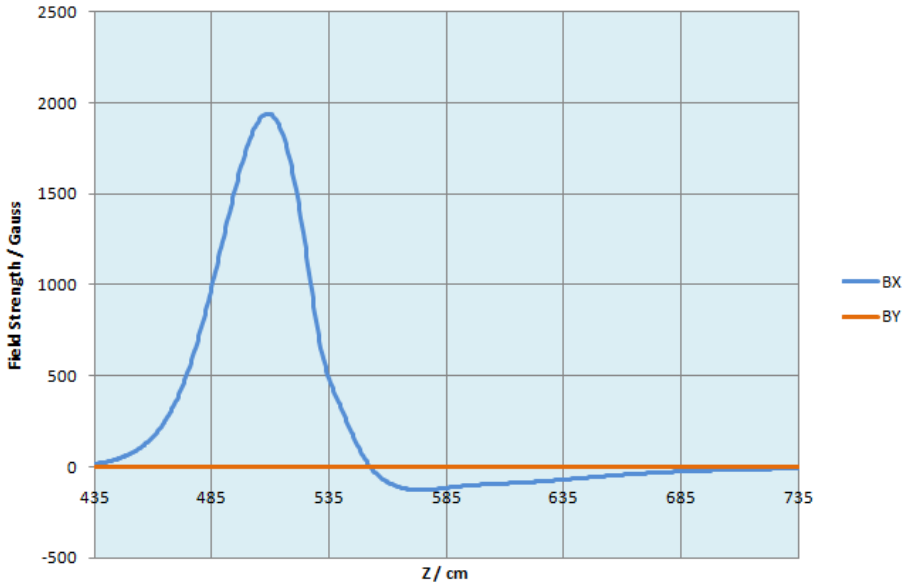

Figure 10: The Magnetic Field from 435 cm to 735 cm.

Fig 11 is the layout of the electron lenses' lattice, which is about 7.412230 m and 7.412232 m long for left side of IP10 and right side of IP10. It replaces the element from AP10P4G to AP10P21G around IP 10. Because there is a vertical field, By, inside the main solenoid (due to a 5 mm offset), the length of this solenoid is reduced to 2.35 m, but the integral values of Bz and L remain constant; the 2.35 long solenoid has the same ks as the 2.5 m solenoids. Appendix A gives more details.

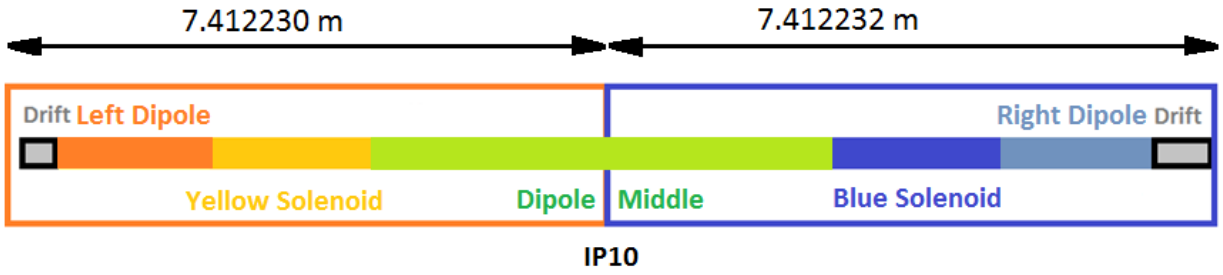

Figure 11: The layout of the electron lens lattice.

5. Closed Orbit Calculation with Simtrack Code

With the Simtrack code, we determined the entire ring's closed orbit including the RHIC lattice that encompasses the electron lenses' lattice: the results are shown in Figure 12 and Figure 13.

For tracking the 2011 Blue 250GeV polarized proton lattice was used. Its tune was set to (28.67, 29.675), and its chromaticity was set to (1.0, 1.0) without head-on beam-beam collisions at IP 6 and IP8. Because of this, the initial angle of the proton beam is set before it goes into the E-lens lattice, this is one reason that the proton beams have different shift between Opera and Simtrack code tracking.

From Figure 12, the vertical proton beam's closed orbit changes 1.3 mm in (-735, 735) cm. IP 10, with its zero coordinate, is the center of the E-lens. For the horizontal plane, the closed orbit changes 0.18 mm. The green lines in Figure 12 and Figure 13 are the closed orbits without the E-lenses' lattice, which have zero transverse offset.

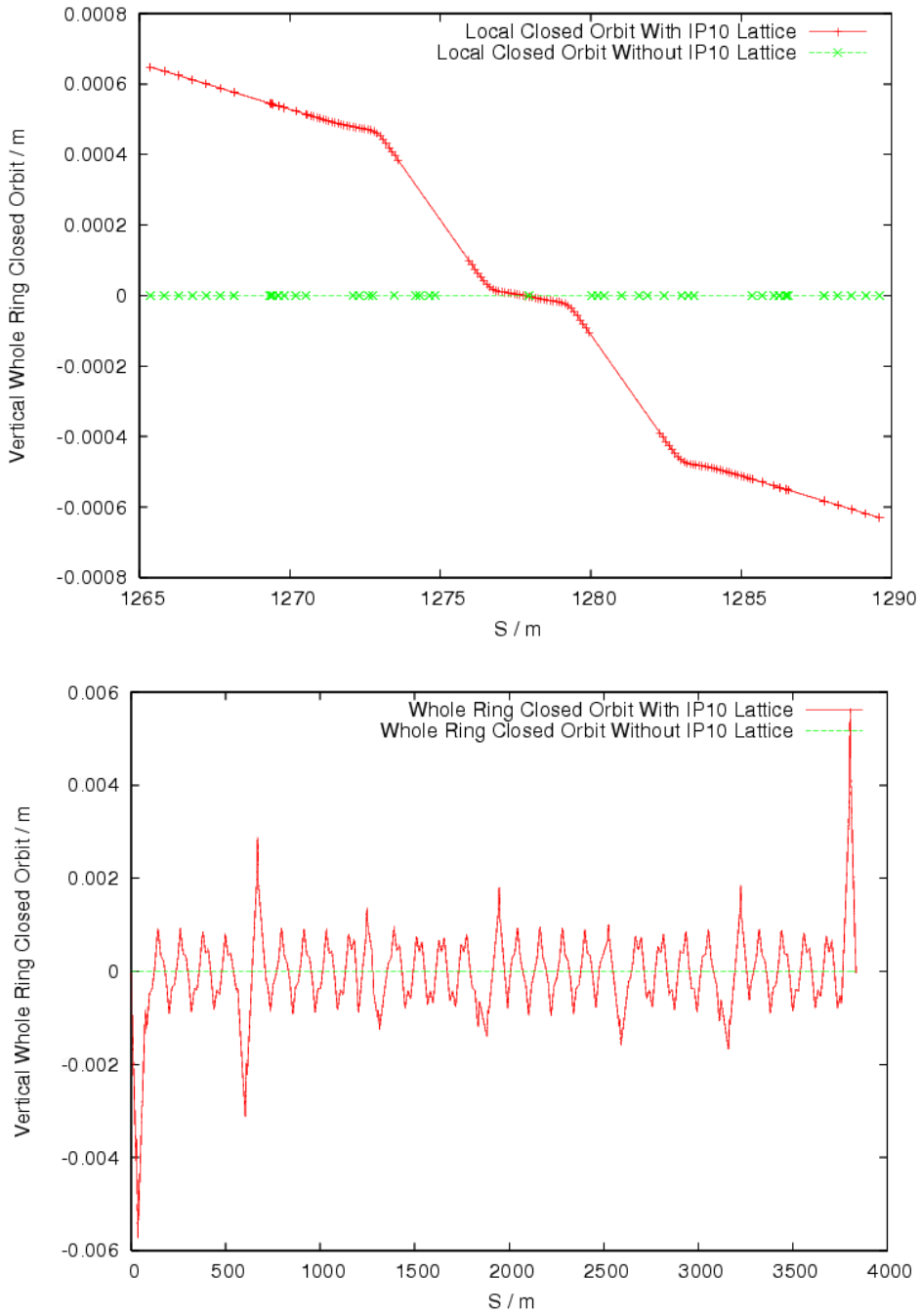

Figure 12: The Vertical Closed Orbit with (Red) and without (Green) the E-lens Lattice.

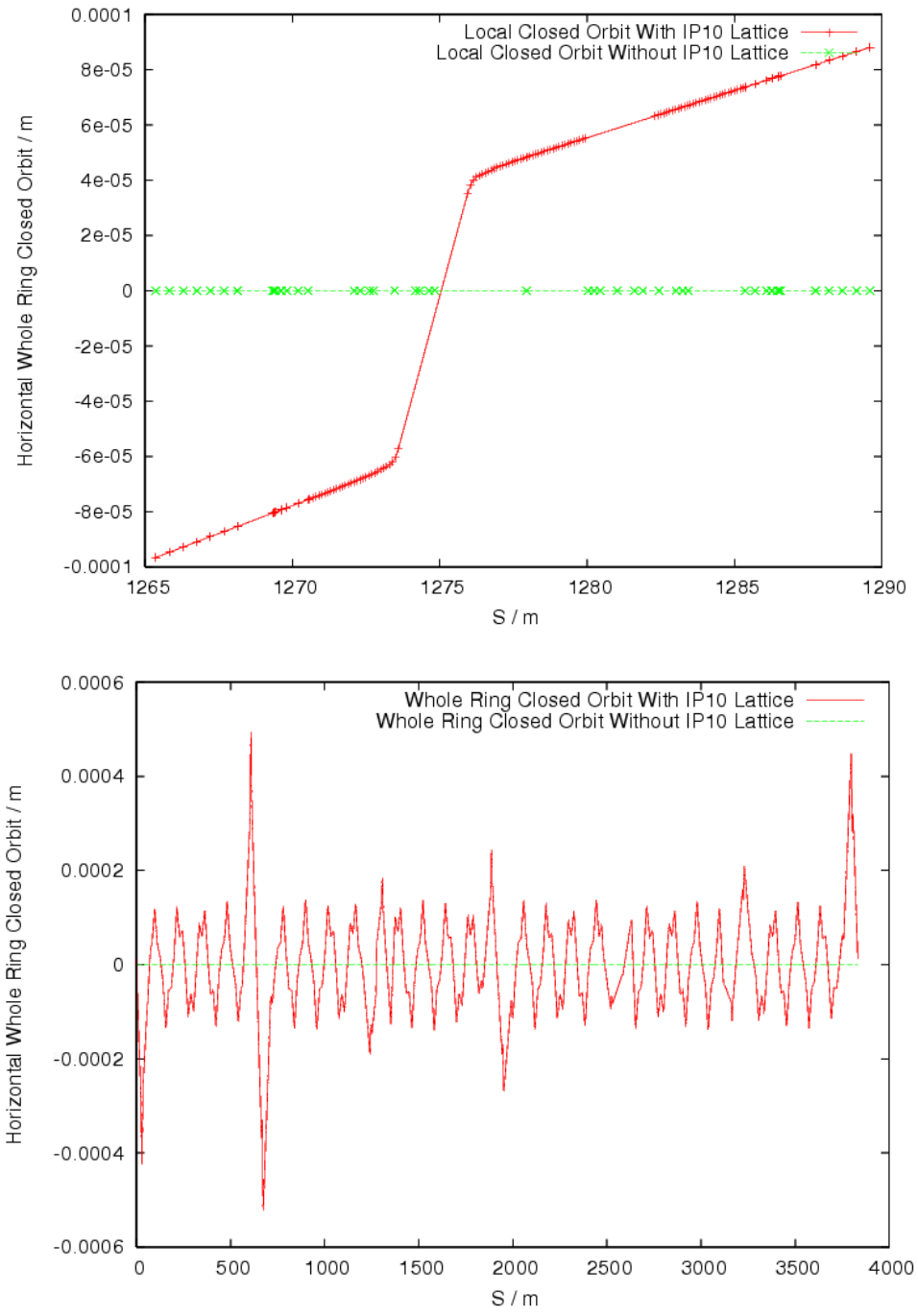

Figure 13: The Horizontal Closed Orbit with (Red) and without (Green) the E-lens Lattice.

Figure 14 and Figure 15 plot, respectively, the horizontal- and vertical-beta function with and without the E-lens lattice. They show no big differences because there is no large quadrupole error introduced.

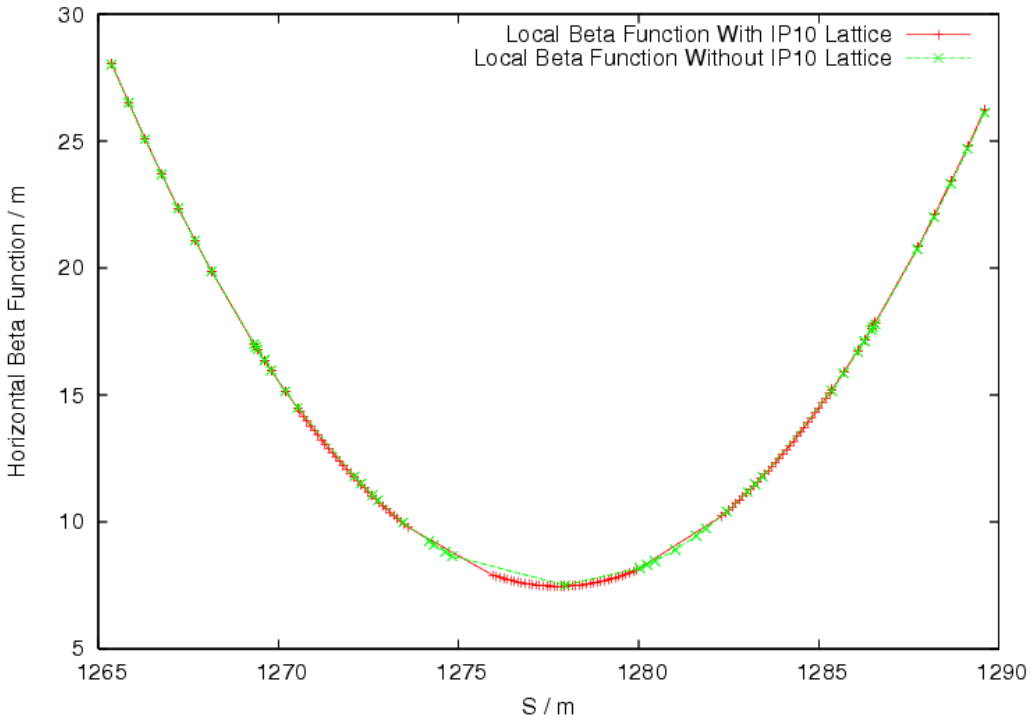

Figure 14: The Horizontal Beta Function with (Red) and without (Green) the E-lenses Lattice.

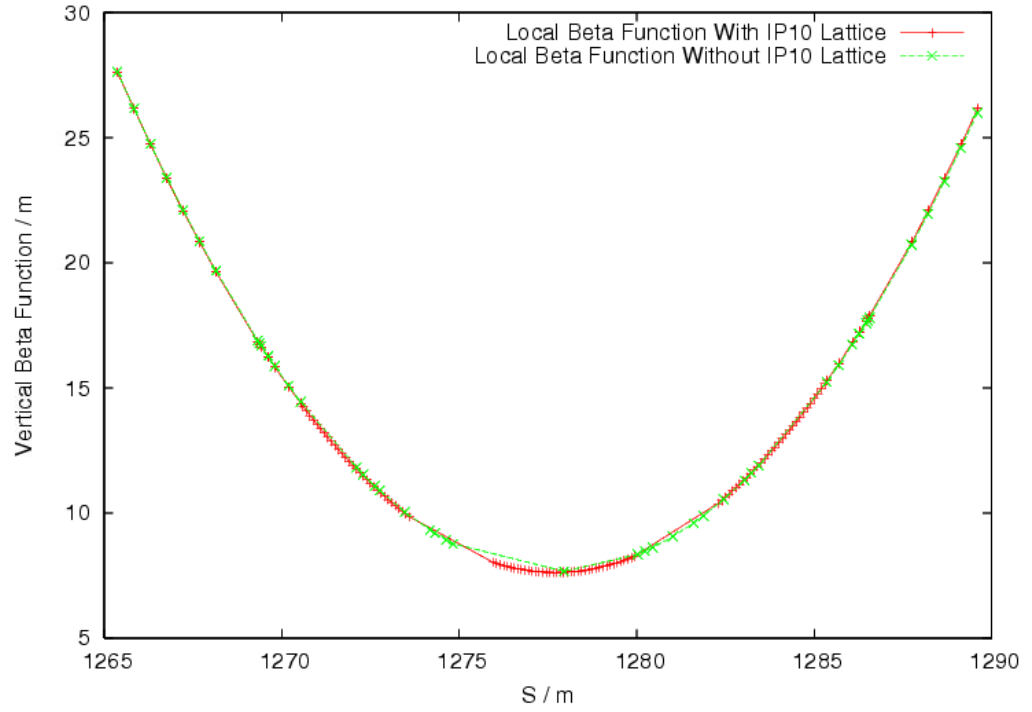

Figure 15: The Vertical Beta Function with (Red) and without (Green) the E-lenses Lattice.

Figure 16 illustrates the phase advance of the elements around IP10 with and without the E-lens for the vertical- and horizontal-plane.

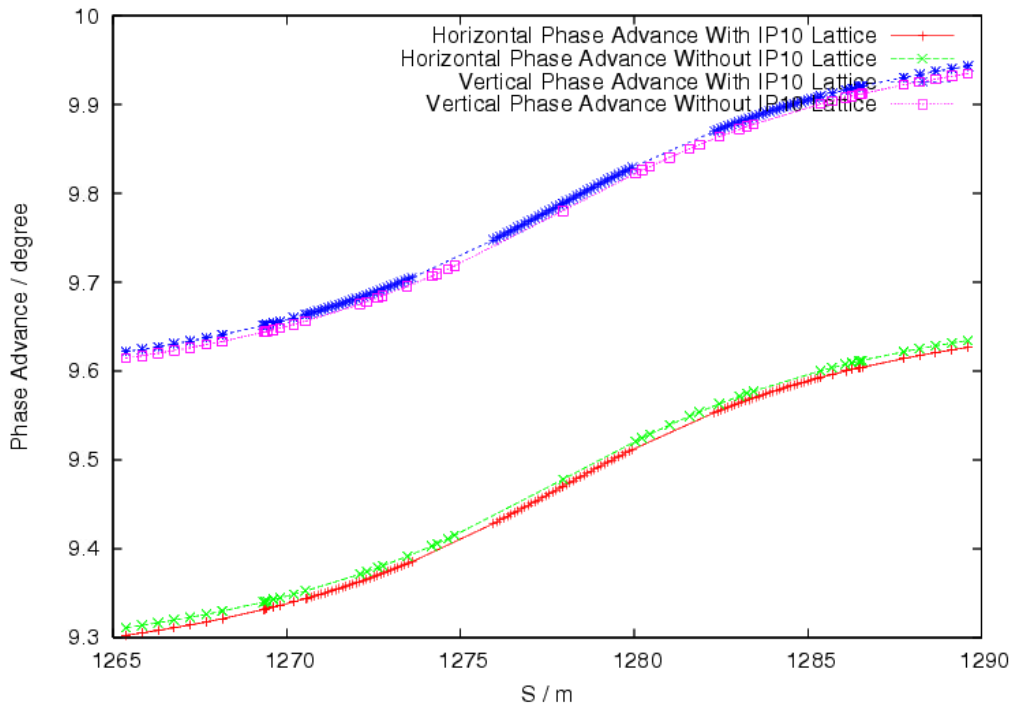

Figure 16: The Phase Advance with (Red and Blue) and without (Green and Magenta) the E-lens Lattice.

Table 1 lists the parameters for the proton beam with and without Elens lattice. The horizontal tune changed 0.0001 and vertical tune changed 0.0003. Other parameters also have no big difference with and without Elens lattice.

Table 1 Proton Beam Parameters With and Without Elens.

Parameters	Without Elens Lattice		With Elens Lattice	
	X	Y	X	Y
Tune	28.6949	29.6849	28.6950	29.6846
Chrom1	0.882692	0.91706	0.811907	0.905909
Chrom2	1867.42	1977.68	1871.67	1962.08
Alpha#	0.714805	0.708052	0.726546	0.71088
Beta#	-0.144506	-0.0409973	-0.191133	0.00453062

that is the twiss parameters at the starting point.

6. Calculation of the E-lens Transport Matrix by Opera

A third method of tracking the proton beam with the E-lenses is by the transport matrix, for example, from -9 m to 9 m around IP10. We also can calculate the transport matrix from -9 m to the inner side of main solenoids, such as -4, -2, 2, and 4 m. Knowing the initial proton beam parameters, we then can determine the beam's parameters inside the superconducting solenoid from these transport matrixes when the E-lens is operating.

To assess these transport matrixes, we used the response matrix calculating method. One initial parameter is changed, for example, the dx in the Table 2, and then Opera calculates the output value dX, dX', dY, and dY' as the function of dx. If these values display a linear function, we can fit them, as in the first column of Figure 17 (Appendix B). Then, we can obtain their coefficients from the fitting, as in the first column of Table.

Table 2: How to Get the Matrix Elements.

Variable	Input	Output
dx	dx	dX/dx
	0	dX'/dx
	-0.005	dY/dx
	0	dY'/dx
dx'	0	dX/dx'
	dx'	dX'/dx'
	-0.005	dY/dx'
	0	dY'/dx'
dy	0	dX/dy
	0	dX'/dy
	dy-0.005	dY/dy
	0	dY'/dy
dy'	0	dX/dy'
	0	dX'/dy'
	-0.005	dY/dy'
	dy'	dY'/dy'

Thereafter, we repeated the calculation for dx', dy, and dy' in Table 1 to get the other three columns in the Table 3. In this manner, we have all the transport matrix elements from -9 to Z (Z may be inside or outside the E-lens).

Table3: The Matrix Elements.

dX/dx	dX/dx'	dX/dy	dX/dy'
dX'/dx	dX'/dx'	dX'/dy	dX'/dy'
dY/dx	dY/dx'	dY/dy	dY/dy'
dY'/dx	dY'/dx'	dY'/dy	dY'/dy'

For the transport matrix from -9 m to 9 m, the transport matrix is

0.9994	17.99	1.00E-05	0.0044
-7.00E-05	0.9993	1.00E-06	-1.00E-05

-8.00E-06	-0.0044	0.9994	-17.991
-7.00E-07	-5.00E-06	-6.00E-05	-1.00E+00

And the constant matrix is

0.000100
0
-0.005629
0

When we use these transport matrixes, the output parameters ([1*4] array) are equal to the transport matrix ([4*4] array) times the input parameters ([1*4] array) plus a constant matrix ([1*4] array).

7. Discussion

In this paper, we discuss our design of the vertical- and horizontal-layout of two RHIC electron lenses. Firstly, we simulated, with Opera, the single pass trajectories of the proton beam in these two electron lenses. With about a 100-μrad initial vertical angle, the proton beam becomes parallel to the Z-axis that is, the axis of the electron beam.

An E-lens lattice is created without considering the higher order magnetic field, and misalignments of its elements. Further, we tracked by the Simtrack code, the entire ring's beam parameters with the 2011 blue 250-GeV polarized proton beam's lattice that includes the E-lens lattice.

Finally, we introduced the transport matrix method as the third method for tracking the proton beam.

These trackings and simulations give us a greater understanding about the proton beam's behavior inside the E-lens, and also afford clues on the alignment between the proton beam and the electron beam when we apply head-on beam-beam compensation.

8. Appendix A

IP 10 Lattice without E-lens			
Element	Location	Length	Type
HDXPM09	1265.37	0.462527	SBEND
HDXPM09M2	1265.37	0	MULT
HDXPM09	1265.84	0.462527	SBEND
HDXPM09M3	1265.84	0	MULT
HDXPM09	1266.3	0.462527	SBEND
HDXPM09M4	1266.3	0	MULT
HDXPM09	1266.76	0.462527	SBEND
HDXPM09M5	1266.76	0	MULT
HDXPM09	1267.22	0.462527	SBEND
HDXPM09M6	1267.22	0	MULT
HDXPM09	1267.69	0.462527	SBEND
HDXPM09M7	1267.69	0	MULT
HDXPM09	1268.15	0.462527	SBEND
HDXPM09M8	1268.15	0	MULT
ELDXPM09	1268.15	0	DRIFT
ODXFLX	1269.33	1.18563	DRIFT
AP10P0G	1269.33	0	MARKER
OBSK9LG	1269.38	0.048623	DRIFT
MVALVE	1269.38	0	MARKER
OX9A0	1269.43	0.04875	DRIFT
AP10P1G	1269.43	0	MARKER
OBXFLA	1269.62	0.1905	DRIFT
BPMH	1269.62	0	HBPM
CPLMON	1269.62	0	BPM
BPMV	1269.62	0	VBPM
OBXFLX	1269.81	0.1905	DRIFT
AP10P2G	1269.81	0	MARKER
OX9A1	1270.2	0.390525	DRIFT
AP10P3G	1270.2	0	MARKER
OX9A2	1270.54	0.333248	DRIFT
AP10P4G	1270.54	0	MARKER
OX9A3	1272.11	1.56947	DRIFT
AP10P5G	1272.11	0	MARKER
OX9A4	1272.3	0.19812	DRIFT
AP10P6G	1272.3	0	MARKER

IP 10 Lattice with E-lens			
Element	Location	Length	Type
HDXPM09	1265.37	0.462527	SBEND
HDXPM09M2	1265.37	0	MULT
HDXPM09	1265.84	0.462527	SBEND
HDXPM09M3	1265.84	0	MULT
HDXPM09	1266.3	0.462527	SBEND
HDXPM09M4	1266.3	0	MULT
HDXPM09	1266.76	0.462527	SBEND
HDXPM09M5	1266.76	0	MULT
HDXPM09	1267.22	0.462527	SBEND
HDXPM09M6	1267.22	0	MULT
HDXPM09	1267.69	0.462527	SBEND
HDXPM09M7	1267.69	0	MULT
HDXPM09	1268.15	0.462527	SBEND
HDXPM09M8	1268.15	0	MULT
ELDXPM09	1268.15	0	DRIFT
ODXFLX	1269.33	1.18563	DRIFT
AP10P0G	1269.33	0	MARKER
OBSK9LG	1269.38	0.048623	DRIFT
MVALVE	1269.38	0	MARKER
OX9A0	1269.43	0.04875	DRIFT
AP10P1G	1269.43	0	MARKER
OBXFLA	1269.62	0.1905	DRIFT
BPMH	1269.62	0	HBPM
CPLMON	1269.62	0	BPM
BPMV	1269.62	0	VBPM
OBXFLX	1269.81	0.1905	DRIFT
AP10P2G	1269.81	0	MARKER
OX9A1	1270.2	0.390525	DRIFT
AP10P3G	1270.2	0	MARKER
OX9A2	1270.54	0.333248	DRIFT
AP10P4G	1270.54	0	MARKER
LDFT_Yellow	1270.6	0.06223	DRIFT
Left Dipole	1270.7	0.1	KICKER
Left Dipole	1270.8	0.1	KICKER
Left Dipole	1270.9	0.1	KICKER

OX9A5	1272.62	0.3175	DRIFT		Left Dipole	1271	0.1	KICKER
AP10P7G	1272.62	0	MARKER		Left Dipole	1271.1	0.1	KICKER
OX9A6	1272.76	0.141986	DRIFT		Left Dipole	1271.2	0.1	KICKER
AP10P8G	1272.76	0	MARKER		Left Dipole	1271.3	0.1	KICKER
OTWHFL1	1273.47	0.707009	DRIFT		Left Dipole	1271.4	0.1	KICKER
TWH	1273.47	0	DRIFT		Left Dipole	1271.5	0.1	KICKER
OTWHFL2	1274.18	0.707009	DRIFT		Left Dipole	1271.6	0.1	KICKER
AP10P9G	1274.18	0	MARKER		Left Dipole	1271.7	0.1	KICKER
OX9A7	1274.32	0.141986	DRIFT		Left Dipole	1271.8	0.1	KICKER
AP10P10G	1274.32	0	MARKER		Left Dipole	1271.9	0.1	KICKER
OX9A8	1274.64	0.3175	DRIFT		Left Dipole	1272	0.1	KICKER
AP10P11G	1274.64	0	MARKER		Left Dipole	1272.1	0.1	KICKER
OX9A9	1274.83	0.19812	DRIFT		Left Dipole	1272.2	0.1	KICKER
AP10P12G	1274.83	0	MARKER		Left Dipole	1272.3	0.1	KICKER
OX9A10	1277.95	3.11353	DRIFT		Left Dipole	1272.4	0.1	KICKER
IP10	1277.95	0	MARKER		Left Dipole	1272.5	0.1	KICKER
OX10A9	1280.03	2.0828	DRIFT		Left Dipole	1272.6	0.1	KICKER
AP10P13G	1280.03	0	MARKER		Left Dipole	1272.7	0.1	KICKER
OX10A8	1280.23	0.19812	DRIFT		Left Dipole	1272.8	0.1	KICKER
AP10P14G	1280.23	0	MARKER		Left Dipole	1272.9	0.1	KICKER
OX10A7	1280.45	0.2159	DRIFT		Left Dipole	1273	0.1	KICKER
AP10P15G	1280.45	0	MARKER		Left Dipole	1273.1	0.1	KICKER
OEDCERNFL	1281.02	0.575056	DRIFT		Left Dipole	1273.2	0.1	KICKER
EDCERN	1281.02	0	DRIFT		Left Dipole	1273.3	0.1	KICKER
OEDCERNFL	1281.6	0.575056	DRIFT		Left Dipole	1273.4	0.1	KICKER
AP10P16G	1281.6	0	MARKER		Left Dipole	1273.5	0.1	KICKER
OX10A6	1281.88	0.279908	DRIFT		Left Dipole	1273.6	0.1	KICKER
AP10P17G	1281.88	0	MARKER		YSOLEN	1275.95	2.35	SOLEN
OEDCERNFL	1282.45	0.575056	DRIFT		Middle	1276.05	0.1	KICKER
EDCERN	1282.45	0	DRIFT		Middle	1276.15	0.1	KICKER
OEDCERNFL	1283.03	0.575056	DRIFT		Middle	1276.25	0.1	KICKER
AP10P18G	1283.03	0	MARKER		Middle	1276.35	0.1	KICKER
OX10A5	1283.24	0.2159	DRIFT		Middle	1276.45	0.1	KICKER
AP10P19G	1283.24	0	MARKER		Middle	1276.55	0.1	KICKER
OX10A4	1283.44	0.19812	DRIFT		Middle	1276.65	0.1	KICKER
AP10P20G	1283.44	0	MARKER		Middle	1276.75	0.1	KICKER
OX10A3	1285.36	1.92126	DRIFT		Middle	1276.85	0.1	KICKER
AP10P21G	1285.36	0	MARKER		Middle	1276.95	0.1	KICKER
OX10A2	1285.69	0.333248	DRIFT		Middle	1277.05	0.1	KICKER
AP10P22G	1285.69	0	MARKER		Middle	1277.15	0.1	KICKER

OX10A1	1286.08	0.390525	DRIFT		Middle	1277.25	0.1	KICKER
AP10P23G	1286.08	0	MARKER		Middle	1277.35	0.1	KICKER
OBXFLX	1286.27	0.1905	DRIFT		Middle	1277.45	0.1	KICKER
BPMH	1286.27	0	HBPM		Middle	1277.55	0.1	KICKER
CPLMON	1286.27	0	BPM		Middle	1277.65	0.1	KICKER
BPMV	1286.27	0	VBPM		Middle	1277.75	0.1	KICKER
OBXFLA	1286.47	0.1905	DRIFT		Middle	1277.85	0.1	KICKER
AP10P24G	1286.47	0	MARKER		Middle	1277.95	0.1	KICKER
OX10A0	1286.51	0.04875	DRIFT		IP10	1277.95	0	MARKER
MVALVE	1286.51	0	MARKER		Middle	1278.05	0.1	KICKER
OBSK10LG	1286.56	0.048623	DRIFT		Middle	1278.15	0.1	KICKER
AP10P25G	1286.56	0	MARKER		Middle	1278.25	0.1	KICKER
ODXFLX	1287.75	1.18563	DRIFT		Middle	1278.35	0.1	KICKER
ELDXMP10	1287.75	0	DRIFT		Middle	1278.45	0.1	KICKER
HDXMP10M0	1287.75	0	MULT		Middle	1278.55	0.1	KICKER
HDXMP10	1288.21	0.462527	SBEND		Middle	1278.65	0.1	KICKER
HDXMP10M1	1288.21	0	MULT		Middle	1278.75	0.1	KICKER
HDXMP10	1288.67	0.462527	SBEND		Middle	1278.85	0.1	KICKER
HDXMP10M2	1288.67	0	MULT		Middle	1278.95	0.1	KICKER
HDXMP10	1289.14	0.462527	SBEND		Middle	1279.05	0.1	KICKER
HDXMP10M3	1289.14	0	MULT		Middle	1279.15	0.1	KICKER
HDXMP10	1289.6	0.462527	SBEND		Middle	1279.25	0.1	KICKER
HDXMP10M4	1289.6	0	MULT		Middle	1279.35	0.1	KICKER
					Middle	1279.45	0.1	KICKER
					Middle	1279.55	0.1	KICKER
					Middle	1279.65	0.1	KICKER
					Middle	1279.75	0.1	KICKER
					Middle	1279.85	0.1	KICKER
					Middle	1279.95	0.1	KICKER
					BSOLEN	1282.3	2.35	SOLEN
					Right Dipole	1282.4	0.1	KICKER
					Right Dipole	1282.5	0.1	KICKER
					Right Dipole	1282.6	0.1	KICKER
					Right Dipole	1282.7	0.1	KICKER
					Right Dipole	1282.8	0.1	KICKER
					Right Dipole	1282.9	0.1	KICKER
					Right Dipole	1283	0.1	KICKER
					Right Dipole	1283.1	0.1	KICKER
					Right Dipole	1283.2	0.1	KICKER
					Right Dipole	1283.3	0.1	KICKER

					Right Dipole	1283.4	0.1	KICKER
					Right Dipole	1283.5	0.1	KICKER
					Right Dipole	1283.6	0.1	KICKER
					Right Dipole	1283.7	0.1	KICKER
					Right Dipole	1283.8	0.1	KICKER
					Right Dipole	1283.9	0.1	KICKER
					Right Dipole	1284	0.1	KICKER
					Right Dipole	1284.1	0.1	KICKER
					Right Dipole	1284.2	0.1	KICKER
					Right Dipole	1284.3	0.1	KICKER
					Right Dipole	1284.4	0.1	KICKER
					Right Dipole	1284.5	0.1	KICKER
					Right Dipole	1284.6	0.1	KICKER
					Right Dipole	1284.7	0.1	KICKER
					Right Dipole	1284.8	0.1	KICKER
					Right Dipole	1284.9	0.1	KICKER
					Right Dipole	1285	0.1	KICKER
					Right Dipole	1285.1	0.1	KICKER
					Right Dipole	1285.2	0.1	KICKER
					Right Dipole	1285.3	0.1	KICKER
					RDFT_Blue	1285.36	0.062232	DRIFT
					AP10P21G	1285.36	0	MARKER
					OX10A2	1285.69	0.333248	DRIFT
					AP10P22G	1285.69	0	MARKER
					OX10A1	1286.08	0.390525	DRIFT
					AP10P23G	1286.08	0	MARKER
					OBXFLX	1286.27	0.1905	DRIFT
					BPMH	1286.27	0	HBPM
					CPLMON	1286.27	0	BPM
					BPMV	1286.27	0	VBPM
					OBXFLA	1286.47	0.1905	DRIFT
					AP10P24G	1286.47	0	MARKER
					OX10A0	1286.51	0.04875	DRIFT
					MVALVE	1286.51	0	MARKER
					OBSK10LG	1286.56	0.048623	DRIFT
					AP10P25G	1286.56	0	MARKER
					ODXFLX	1287.75	1.18563	DRIFT
					ELDXMP10	1287.75	0	DRIFT
					HDXMP10M0	1287.75	0	MULT
					HDXMP10	1288.21	0.462527	SBEND

					HDXMP10M1	1288.21	0	MULT
					HDXMP10	1288.67	0.462527	SBEND
					HDXMP10M2	1288.67	0	MULT
					HDXMP10	1289.14	0.462527	SBEND
					HDXMP10M3	1289.14	0	MULT
					HDXMP10	1289.6	0.462527	SBEND
					HDXMP10M4	1289.6	0	MULT

Appendix B

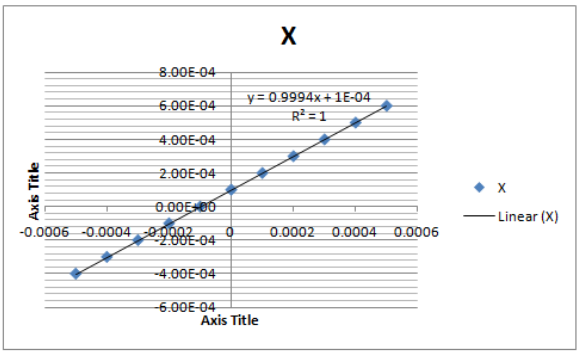
X
y = 0.9994x + 1E-04
R² = 1
Axis Title
X
Linear (X)

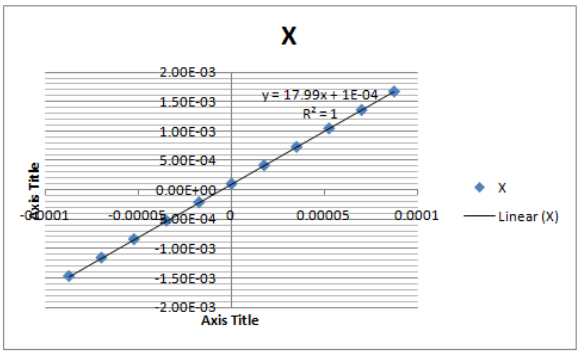
X
y = 17.99x + 1E-04
R² = 1
Axis Title
X
Linear (X)

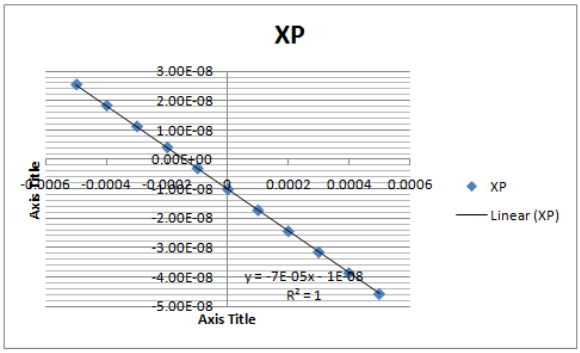
XP
y = -7E-05x - 1E-08
R² = 1
Axis Title
XP
Linear (XP)

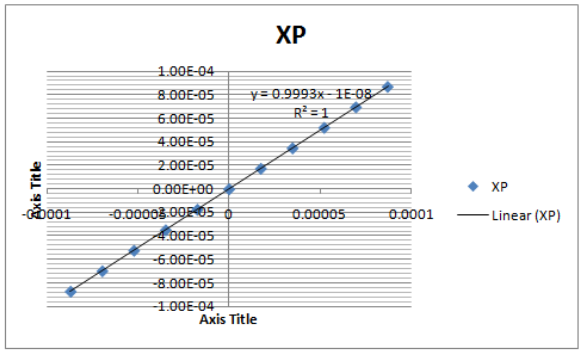
XP
y = 0.9993x - 1E-08
R² = 1
Axis Title
XP
Linear (XP)

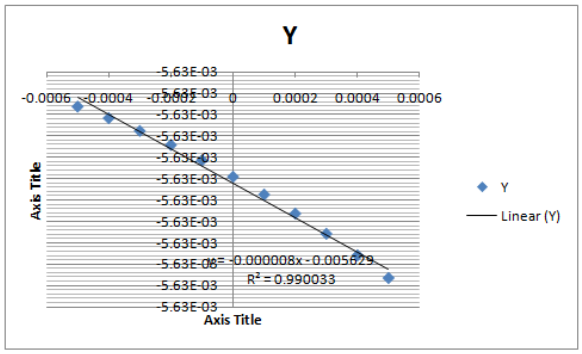
Y
y = -0.000008x - 0.005629
R² = 0.990033
Axis Title
Y
Linear (Y)

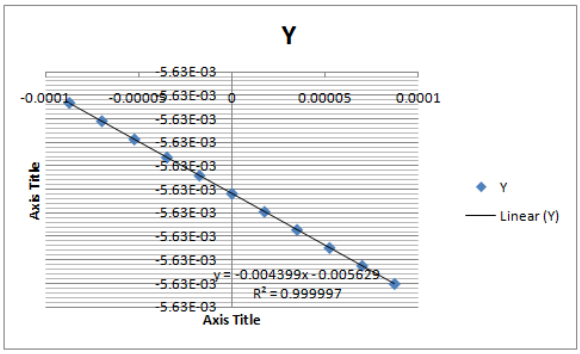
Y
y = -0.004399x - 0.005629
R² = 0.999997
Axis Title
Y
Linear (Y)

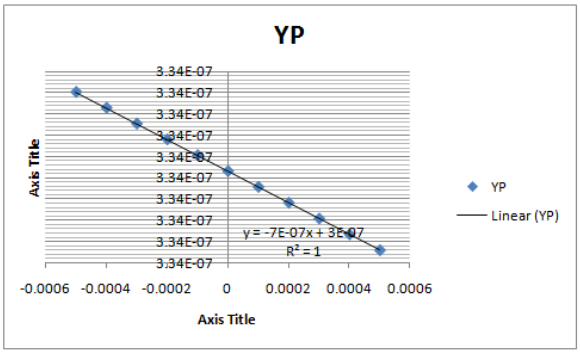
YP
y = -7E-07x + 3E-07
R² = 1
Axis Title
YP
Linear (YP)

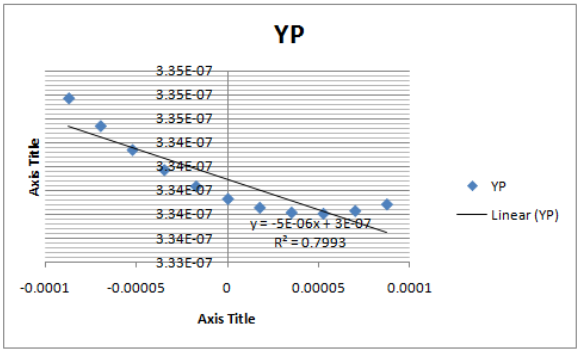
YP
y = -5E-06x + 3E-07
R² = 0.7993
Axis Title
YP
Linear (YP)

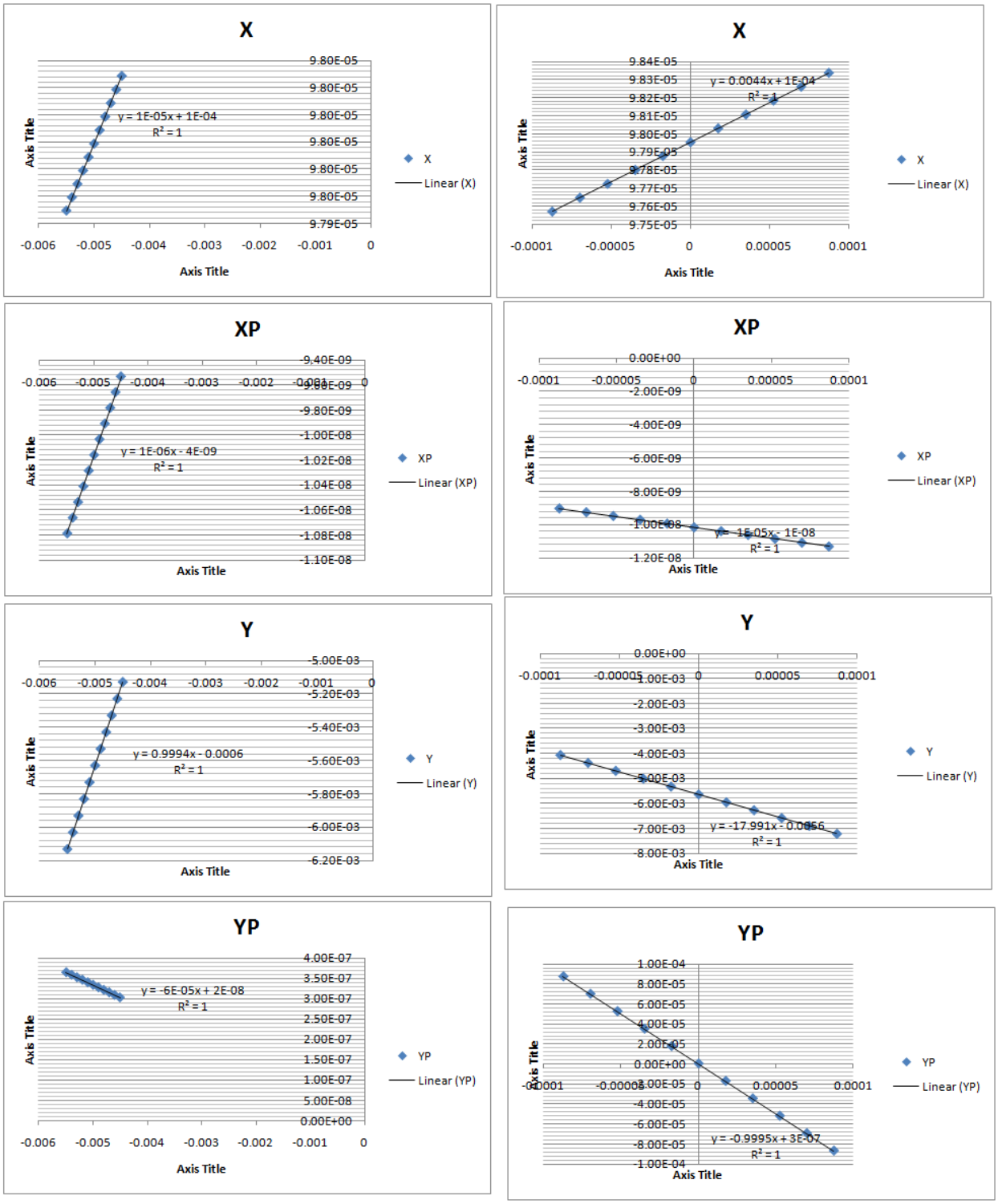

Figure 17: Fitting the function, and obtaining the coefficients.